PS/AA/ACOL Note 53 23 August 1987
MRH/afm

COMPUTED EFFECTS OF SHIMS AT THE END OF THE AC BHN DIPOLES

M.R. Harold

INTRODUCTION

Magnet programmes TOSCA and PE2D have been used in an attempt to predict the effects of shims placed at the ends of the BHN dipoles in the AC. Because only comparisons were required (with and without shim) the pole shape was only approximately represented (see Fig. 1). Even with this simplified geometry, obtaining consistent results from TOSCA proved difficult.

MAGNET REPRESENTATION

The pole shape is shown in Fig. 1; the major difference from reality is that the pole corners are not rounded. A single shim 6 mm thick, 27 mm wide and 75 mm high was moved in steps of 27 mm so as to cover the whole of one half of the pole end. The field integrals through the magnet were computed for x = -105 to x = 105 mm in steps of 15 mm with the intention of comparing them with the "no shim" case.

Because magnetic saturation is appreciable at pole-ends, the different cases were all run in the non-linear mode, the B-H curve employed being the same as that used for Q54. The half-length of the yoke as represented in TOSCA was 10 mm less than the actual half-length.

RESULTS

For unknown reason the problem was very reluctant to converge, and eventually most of the cases were terminated after 30 iterations, still unconverged. In order that the jobs should run overnight, they were split into two runs of 15 iterations each. TOSCA has always had the peculiarity that on re-starting from an old solution, the initial iterations fluctuate wildly so that after the second series of 15 iterations one is not much nearer convergence than before. Cases BHN3-BHN6 (shim covering x = 0 to 108 mm) were run in this way, and as can be seen from the fields at z = 0 (Table 1) good consistency was found.

For cases BHN7 (shim at -135 to -108 mm) and BHN8 (no shim), however, it was not possible to re-start from the old solution without a divide zero error occurring. This was particularly unfortunate in the BHN8 case, since this was to form the base from which all comparisons were to be made. However, after only 15 iterations (16 for BHN7) the fields at z = 0 were found to be sufficiently close to those of cases BHN3-BHN6 that reasonable confidence could be placed in the results, which were obtained as followx:

1. Check that the fields at z = 0 are similar for all cases.

2. Calculate $L_0 = (\int Bdz)/B_0$ at x = 0. These are seen to be consistent in that L_0 increases as the shim is moved towards x = 0.

3. For each case calculate $\Delta L/L_0$ versus x.

4. For BHN3-BHN7 calculate $(\Delta L/L_0) - (\Delta L/L_0)_{BHN8}$ and adjust the base line so that all differences are positive. These are plotted in Fig. 2.

5. For BHN7, and perhaps BHN6, where the shim is far from x = 0, a better result is probably obtained by calculating $(\Delta L/L_0)_{-x}-(\Delta L/L_0)_{+x}$. This too is shown in Fig. 2.

Finally, the effect of a 27 mm-wide bump on the pole profile was computed in 2 dimensions using PE2D. The bump was placed symmetrically about x = 0, and the results processed as follows:

1. Calculate $\Delta B/B_0$ versus x (no bump).
2. Calculate $\Delta B/B_0$ versus x (with bump).
3. Subtract (1) from (2) amd normalise so that $(\Delta B/B_0)_{max} \approx 9,5*E-4$.

This result is included in Fig. 2 (BHN3); it can be seen that a vertically extended shim at the pole-end has a wider radial influence than that of a bump of the same width in the two-dimensional profile.

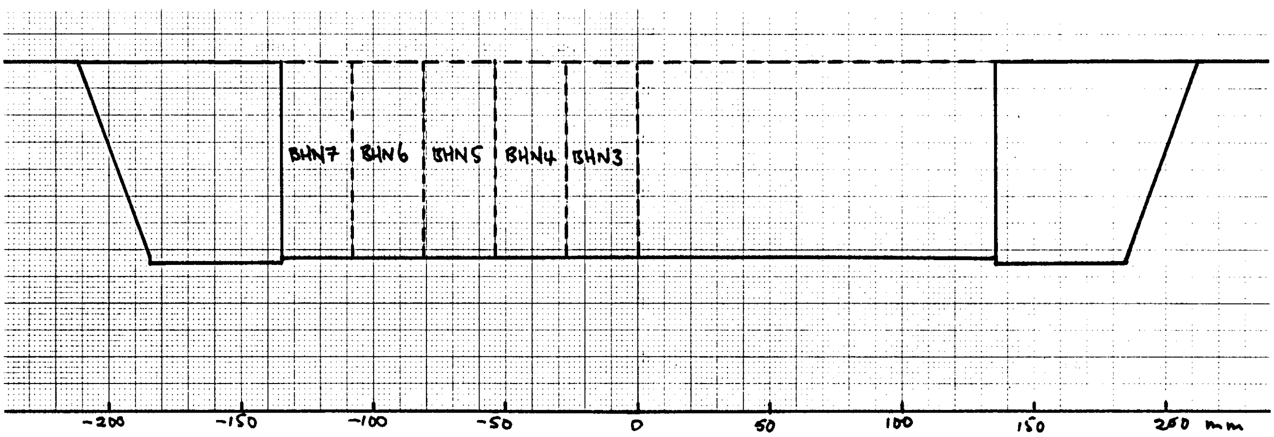

Fig. 1

Table 1.

Case	x(mm)	B(z=0)	$\Delta B/B_0$ *E4	$\int B dz$(g-cm)	$\Delta L/L_0$ *E4	Shim Effect $\Delta L/L_0$ *E4
	-105	14887	42	1442310	31	
	-90	14846	14	1438830	7	
	-75	14821	-3	1436760	-7	
	-60	14814	-7	1436300	-10	
	-45	14815	-7	1436560	-9	
BHN8	-30	14823	-1	1437500	-2	
L =	-15	14823	-1	1437520	-2	
969.85	0	14825	0	1437800	0	
	15	14823	-1	1437520	-2	
	30	14823	-1	1437500	-2	
	45	14815	-7	1436560	-9	
	60	14814	-7	1436300	-10	
	75	14821	-3	1436760	-7	
	90	14846	14	1438830	7	
	105	14887	42	1442310	31	
	-105	14880	40	1441960	34	7
	-90	14840	13	1438530	10	7
	-75	14815	-4	1436440	-4	7
	-60	14809	-8	1435660	-8	6
	-45	14811	-7	1436000	-7	6
BHN7	-30	14819	-1	1436840	-1	5
L =	-15	14819	-1	1436800	-2	4
969.60	0	14821	0	1437040	0	4
	15	14819	-1	1436730	-2	4
	30	14819	-1	1436670	-3	3
	45	14811	-7	1435690	-9	4
	60	14809	-8	1435370	-12	2
	75	14815	-4	1435740	-9	2
	90	14840	13	1437650	4	1
	105	14880	40	1440930	27	0
	-105	14886	39	1443470	36	8
	-90	14847	13	1440140	13	9
	-75	14823	-3	1438130	-1	10
	-60	14817	-7	1437590	-5	8
	-45	14818	-7	1437670	-5	7
BHN6	-30	14827	-1	1438360	0	5
L =	-15	14826	-1	1438200	-1	4
970.00	0	14828	0	1438320	0	3
	15	14826	-1	1437940	-3	2
	30	14826	-1	1437830	-3	2
	45	14817	-7	1436820	-10	2
	60	14816	-8	1436500	-13	0
	75	14823	-3	1436900	-10	0
	90	14848	13	1438900	4	0
	105	14890	42	1442310	28	0
	-105	14886	40	1443250	32	6
	-90	14847	14	1440070	10	8
	-75	14823	-2	1438200	-3	9
	-60	14817	-6	1437800	-5	10
	-45	14818	-5	1437990	-4	10
BHN5	-30	14827	-1	1438780	1	8
L =	-15	14826	0	1438560	0	7
970.31	0	14826	0	1438580	0	5
	15	14826	0	1438120	-3	4
	30	14826	0	1437930	-5	2
	45	14817	-6	1436900	-12	2
	60	14816	-7	1436550	-14	1
	75	14823	-2	1436930	-11	1
	90	14848	15	1438930	2	0
	105	14890	43	1442330	26	0
	-105	14886	39	1442840	27	4
	-90	14847	13	1439760	5	6
	-75	14823	-3	1438020	-7	8
	-60	14817	-7	1437760	-9	9
	-45	14818	-7	1438090	-6	11
BHN4	-30	14827	-1	1439020	0	10
L =	-15	14826	-1	1438900	-1	9
970.47	0	14828	0	1439020	0	8
	15	14826	-1	1438460	-4	6
	30	14826	-1	1438180	-6	4
	45	14817	-7	1437050	-14	3
	60	14816	-8	1436640	-17	1
	75	14823	-3	1437000	-14	1
	90	14848	13	1438980	0	0
	105	14890	42	1442370	23	0
	-105	14886	39	1442550	23	1
	-90	14847	13	1439380	1	3
	-75	14823	-3	1437610	-11	5
	-60	14817	-7	1437450	-13	6
	-45	14818	-7	1437910	-9	9
BHN3	-30	14827	-1	1438970	-2	9
L =	-15	14826	-1	1439000	-2	9
970.64	0	14828	0	1439260	0	9
	15	14826	-1	1438810	-3	8
	30	14826	-1	1438590	-5	6
	45	14817	-7	1437370	-13	5
	60	14816	-8	1436870	-17	2
	75	14823	-3	1437140	-15	1
	90	14848	13	1439070	-1	1
	105	14890	42	1442430	22	0

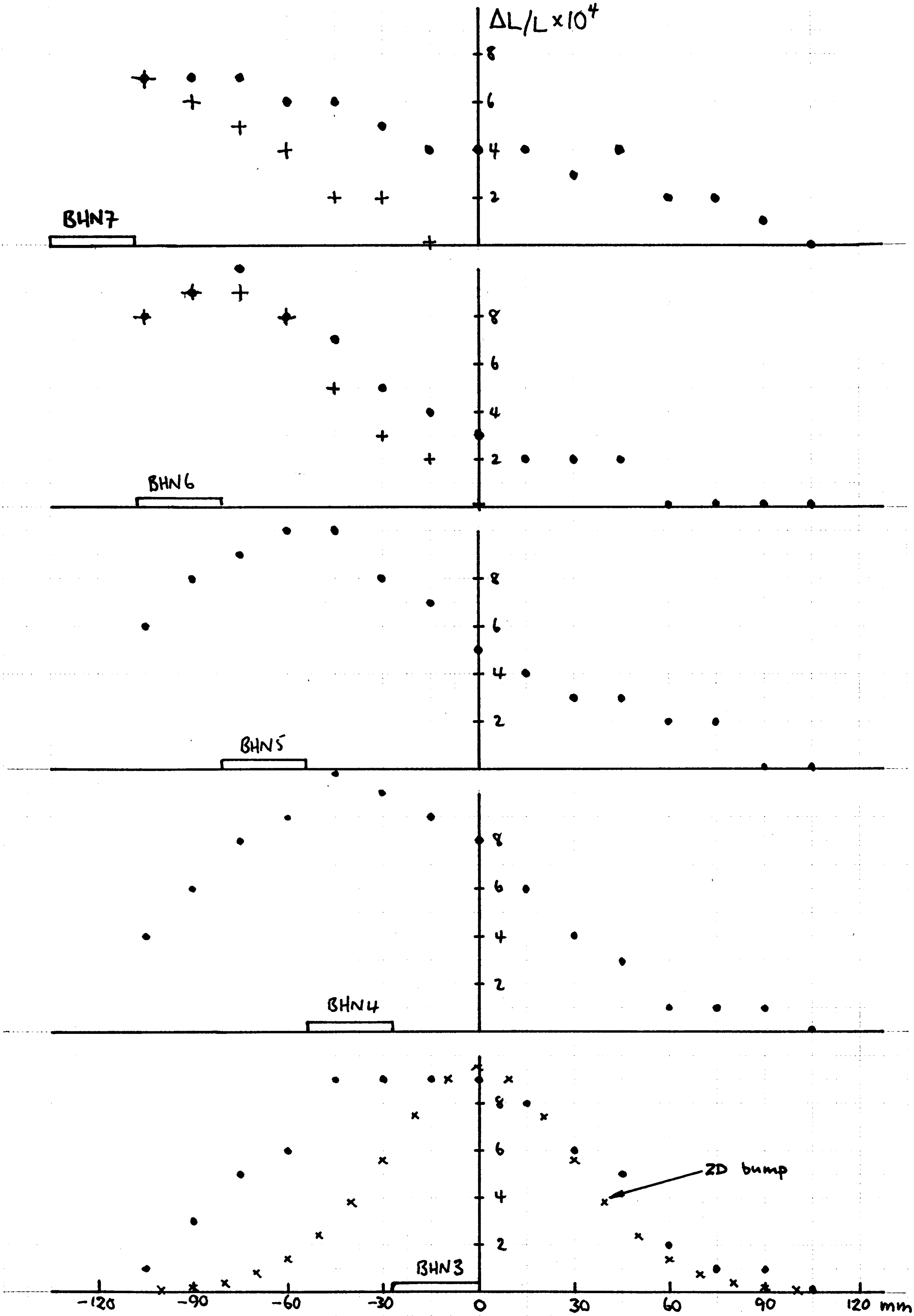

ΔL/L ×10⁴
BHN7
BHN6
BHN5
BHN4
BHN3
2D bump
-120
-90
-60
-30
0
30
60
90
120 mm

Fig. 2.